2019/08/05
Archive Hash: 065da00
Archive Date: 2019/08/05

Search for a narrow resonance decaying to a pair of muons in proton-proton collisions at 13 TeV

The CMS Collaboration

Abstract

A search is presented for a narrow resonance decaying to a pair of muons using 13 TeV proton-proton collision data recorded by the CMS experiment at the CERN LHC. The search in the $45-75$ and $110-200$ GeV resonance mass ranges uses fully reconstructed event data, corresponding to an integrated luminosity of 137 fb^{-1}. The search in the $11.5-45.0$ GeV mass range uses 96.6 fb^{-1} of data collected using a dedicated set of high rate dimuon triggers with low thresholds, which store a reduced amount of trigger level information. No significant resonant peaks are observed. The search sets the strongest constraints on a hypothetical dark photon heavier than 11.5 GeV.

We present a search for a narrow resonance decaying to a pair of muons using 13 TeV proton-proton (pp) collision data recorded by the CMS experiment at the CERN LHC. The search looks for a narrow peak in the dimuon mass distribution. Resonance masses in the range 11.5–200 GeV are probed. The mass range of 75–110 GeV, which is dominated by the Z boson resonance, is omitted. The results of this search are interpreted in the context of a dark photon (Z_D) that may feebly couple the standard model (SM) particles to a hidden, dark sector of particles. The dark photon interacts with SM particles through the kinetic mixing of its $U(1)_D$ gauge field with the $U(1)_Y$ hypercharge field of the SM [1–3]. The degree of this mixing, and consequently, the strength of the coupling of Z_D with SM fermions is determined by the kinetic mixing coefficient ϵ. An extensive discussion of the theory of kinetic mixing, its impact on the electroweak symmetry breaking, and consequently, on the electroweak precision observables can be found in Ref. [4]. Constraints have been placed on visible Z_D decays in direct searches by beam dump [5], fixed target [6], rare meson decay [7], and collider [8, 9] experiments.

The central feature of the CMS apparatus is a superconducting solenoid of 6 m internal diameter, providing a magnetic field of 3.8 T. Within the solenoid volume are a silicon pixel and strip tracker, a lead tungstate crystal electromagnetic calorimeter, and a brass and scintillator hadron calorimeter, each composed of a barrel and two endcap sections. Forward calorimeters extend the pseudorapidity coverage provided by the barrel and endcap detectors. Muons are detected in gas-ionization chambers embedded in the steel flux-return yoke outside the solenoid. A more detailed description of the CMS detector, together with a definition of the coordinate system used and the relevant kinematic variables, can be found in Ref. [10].

Events of interest are selected using a two-tiered trigger system [11]. The first level (L1), composed of custom hardware processors, uses information from the calorimeters and muon detectors to select events at a rate of around 100 kHz within a time interval of less than 4 μs. The second level, known as the high-level trigger (HLT), consists of a farm of processors running a version of the full event reconstruction software optimized for fast processing. A set of triggers in the HLT system reduces the event rate to around 1 kHz at which data containing all the information necessary for complete event reconstruction are transferred to storage. We refer to these triggers as 'standard triggers' in this Letter. The standard dimuon triggers have transverse momentum (p_T) requirements of 12–15 GeV on the highest-p_T muon, and 5–7 GeV on the second highest-p_T muon reconstructed in the L1 step. These events are further reconstructed in the HLT step, where a $p_T > (8)17$ GeV requirement is imposed on the (second) highest-p_T muon candidate. The data collected with the standard dimuon triggers at a rate of about 40 Hz are then fully reconstructed and used in the search probing dimuon resonance masses greater than 45 GeV. Dimuon events that do not fire the standard dimuon triggers, but are instead selected by the single muon triggers with p_T thresholds of 24 (27) GeV during the 2016, 2018 (2017) data-taking periods, are also included. The data collected during the years 2016, 2017 and 2018 correspond to an integrated luminosity of 137 fb^{-1}.

For dimuon resonance masses below $\sim$40 GeV, the p_T thresholds in the standard dimuon triggers significantly reduce the signal acceptance, thereby adversely affecting the search sensitivity. Therefore, a dedicated set of triggers with significantly lower muon p_T thresholds have been implemented. Events selected with these triggers contain a very limited amount of information about muon and other candidate objects reconstructed in the HLT step. This helps to substantially reduce the event size, thereby allowing these triggers to operate at a significantly higher rate compared to the standard triggers. We refer to this approach as 'data scouting' [12], and the high rate triggers are termed 'scouting triggers'. The scouting dimuon triggers collected data in 2017 (2018) at an average rate of 5.6 (4.4) kHz.

The scouting triggers include a L1 trigger requiring two muons with $p_T > 4$ (4.5) GeV and $\Delta R = \sqrt{\Delta\eta^2 + \Delta\phi^2} < 1.2$ for data collected in 2017 (2018). Furthermore, a L1 trigger requiring a pair of muon candidates with $p_T > 4.5$ GeV, $|\eta| < 2.0$, forming an invariant mass between 7 and 18 GeV, is added. Lastly, events passing the standard L1 dimuon triggers are also included. All events passing this suite of L1 triggers are further reconstructed in the HLT step that requires two muons with $p_T > 3$ GeV. Most of the detector information in the selected events is discarded prior to storage. However, events do contain information about the kinematic properties and quality of the muons reconstructed in the HLT step. The data collected using the scouting dimuon triggers in the years 2017 and 2018 correspond to an integrated luminosity of 96.6 fb^{-1}.

The dark photon signal is simulated at leading order (LO) using the Hidden Abelian Higgs Model (HAHM v3) [4, 13] implemented with the MADGRAPH5_aMC@NLO 2.2.2 (2.4.2) generator [14] for the 2016 (2017, 2018) era samples. The width and cross section of the signal process is directly proportional to ϵ^2. The analysis does not rely on simulation for background estimation. However, simulations of certain SM processes are used to evaluate data-to-simulation corrections and corresponding uncertainties in the signal prediction. The process involving the production of the Y(1S) resonance, and its decay to a pair of muons is simulated at LO with PYTHIA 8.230 [15]. The Drell-Yan background is simulated at LO as well as next-to-leading order (NLO) using MADGRAPH5_aMC@NLO. The LO samples are generated with up to four additional partons in the final state, whereas the NLO samples are produced with up to two additional partons in the final state.

Events simulated at the matrix element level for the signal and background processes are then interfaced with PYTHIA in order to simulate the fragmentation, parton shower and hadronization of partons in the initial and final states along with the underlying event. This is done using the CUETP8M1 (CP5) tune [16, 17] in the 2016 (2017, 2018) era simulations. Jets from LO (NLO) simulations performed with the MADGRAPH5_aMC@NLO generator are matched to the parton shower produced by PYTHIA following the MLM (FxFx) prescription [18, 19]. The 2016 (2017, 2018) era simulations use the NNPDF 3.0 (3.1) parton distribution functions [20, 21]. The interactions of all final state particles with the CMS detector are simulated using GEANT 4 [22]. The simulated events include the contribution of particles from additional pp interactions within the same or nearby bunch crossings (pileup), with the multiplicity of reconstructed primary vertices matching that in data.

Events selected with the standard triggers are reconstructed using the particle-flow (PF) algorithm [23]. It aims to reconstruct and identify each individual particle in an event, with an optimized combination of information from the various elements of the CMS detector. Muons are reconstructed by associating a track reconstructed in the tracking detectors with a track in the muon system. The muon momentum is obtained from the curvature of its track. Primary vertices are reconstructed from charged particle tracks in the event, and the vertex with the largest value of summed physics-object p_T^2 is taken to be the primary pp interaction vertex. Hadronic jets are clustered from PF candidates using the anti-k_T algorithm [24, 25] with a distance parameter of 0.4. Jets are identified to originate from b quarks using a deep neural network discrimininant (deepCSV) that takes as input tracks displaced from the primary interaction vertex, identified secondary vertices, jet kinematic variables, and information related to the presence of soft leptons in the jet [26]. A working point on the output of the deepCSV discriminant is chosen such that the probability of misidentifying a light-flavor jet with $p_T > 30$ GeV as a b-quark jet is about 1%.

For the search employing the standard muon triggers and using complete event reconstruction,

events are required to contain at least one well-identified primary vertex, and two oppositely charged muons with p_T greater than 20 and 10 GeV, and $|\eta| < 1.9$, that are geometrically matched to the HLT muon candidates. In events selected with the single muon triggers the muon p_T threshold is set to 26 (29) GeV for data collected in 2016 (2017, 2018). The muons are required to pass certain selection requirements based on the quality of their reconstructed tracks. The absolute values of the transverse and longitudinal impact parameters of the muon tracks are required to be less than 0.2 and 0.5 cm, respectively. The muon isolation, computed as the scalar sum of the p_T of PF photons, charged and neutral PF hadrons, within a cone of radius $\Delta R = \sqrt{\Delta\eta^2 + \Delta\phi^2} = 0.4$ around the direction of the muon momentum, is required to be less than 15% of the muon p_T. Charged PF hadrons not associated with the primary interaction vertex are ignored in this sum. A further correction is applied to the isolation sum in order to subtract the contribution of neutral particles from pileup. Events containing a b-tagged jet with $p_T > 30\,\text{GeV}$ and $|\eta| < 2.4$ are vetoed to suppress the top quark background.

For the search performed using the dimuon scouting triggers, events are required to contain two oppositely charged muons with $p_T > 4\,\text{GeV}$ and $|\eta| < 1.9$, that form a vertex. The muons are required to pass selection requirements based on the track quality information available in the event. The muon isolation, computed as the sum of the p_T of all tracks in a ΔR cone of radius 0.3 around the direction of the muon, is required to be less than 15% of the muon p_T. In order to suppress the background involving nonprompt muons that typically have low p_T, the (second) highest-p_T muon is required to have $p_T >$ (dimuon mass)/3(4).

Figure 1 shows the dimuon invariant mass distributions obtained with data collected using the standard and scouting dimuon triggers. The dimuon mass distribution of fully reconstructed events collected using the standard triggers suffers from significant acceptance loss, and therefore bends and dips as the dimuon mass goes lower than ~40 GeV. The loss of acceptance is due to the p_T thresholds of 20 and 10 GeV on the two muons. The dimuon mass distribution of events collected using scouting triggers, however, continues to rise steadily for masses lower than 40 GeV. For masses lower than 20 GeV, we see an even steeper rise. This is the region where the L1 triggers with a requirement for the dimuon mass to be in the range 7–18 GeV contribute significantly.

The dimuon mass resolution depends strongly on the $|\eta|$ of the two muons. The p_T resolution of muons in the central barrel region of the detector ($|\eta| < 0.9$) is around 1% for muons with $p_T < 50\,\text{GeV}$, whereas the p_T resolution of muons in endcaps of the muon system ($|\eta| > 1.2$) is around 3% [27]. Therefore, events are divided in two categories. The barrel category consists of events in which both muons have $|\eta| < 0.9$, and the forward category involves events in which at least one of the two muons has $0.9 < |\eta| < 1.9$.

The intrinsic width of the signal resonance considered in this search is assumed to be much narrower than the detector resolution. The signal line shape is modeled using a parametric shape called the double-sided Crystal Ball function [28]. The core of the dCB function consists of the Gaussian distribution of mean s and standard deviation σ. The s and σ parameters represent the peak position and resolution of the resonance, and are allowed to vary using constrained nuisance parameters corresponding to the muon momentum scale and resolution uncertainties. The uncertainty in the dimuon mass resolution is estimated to be 10% of σ. The uncertainty in the mass scale is taken to be 0.1% of the resonance mass in the search performed using data from standard triggers, while it varies between 0.06–0.13% for the search performed using data from the scouting triggers.

There are several experimental sources of systematic uncertainty in the estimation of the signal yield. The measured integrated luminosity has an uncertainty of 2.5% (2.3%) for data taken in

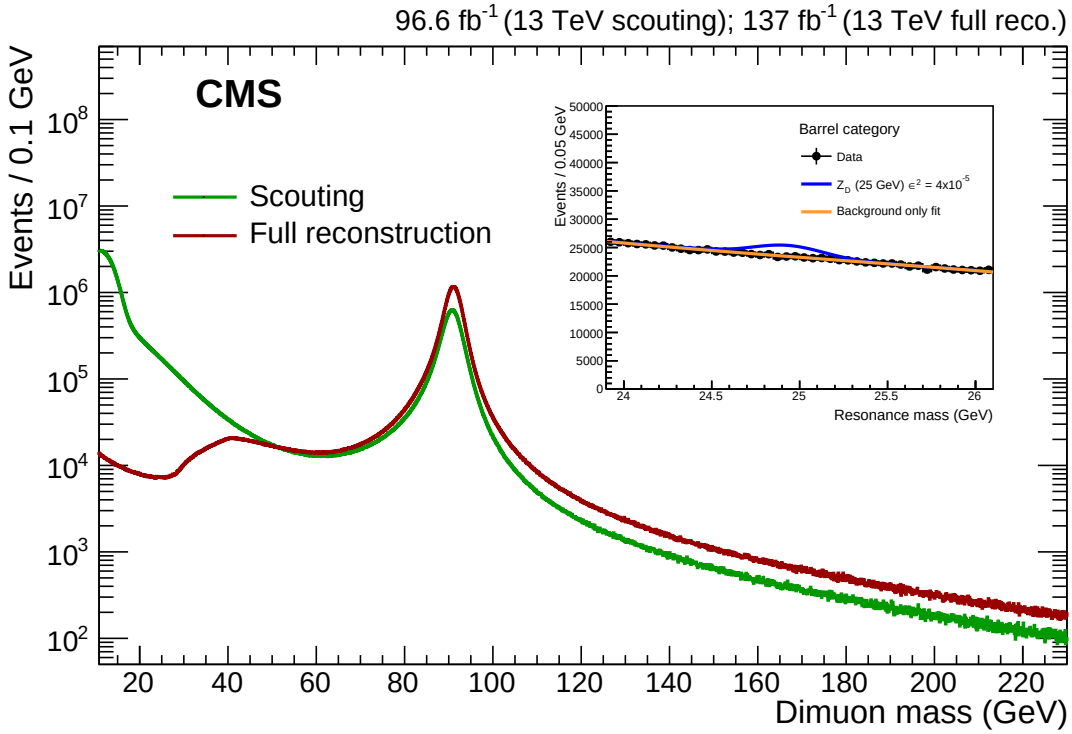

Figure 1: Dimuon invariant mass distributions of events selected with the standard and scouting dimuon triggers. Events are required to pass all the selection requirements. The distribution shown in red corresponds to the data collected using the standard triggers, corresponding to a total integrated luminosity of 137 fb^{-1}. The distribution shown in green corresponds to the data collected using the scouting muon triggers, corresponding to a total integrated luminosity of 96.6 fb^{-1}. The inset figure shows the dimuon mass distribution of events in the barrel category in the mass range $23.9 - 26.1$ GeV. A function describing the background is fit to this data and a 25 GeV dark photon signal corresponding to $\epsilon^2 = 4 \times 10^{-5}$ is added.

2016, 2018 (2017) [29–31]. The uncertainty in the modeling of the pileup conditions is estimated to be 2.5%. In the search performed using the standard muon triggers, uncertainties of 0.2% and 1.5–3.0% are ascribed to the measurement of the trigger and muon selection efficiencies, respectively. The uncertainty in the inefficiency caused by the b jet veto is 1%. In the search performed using scouting data, the uncertainty in the muon selection efficiency varies between 3–10%. The uncertainty in the trigger efficiency is found to be less than 5% for dimuon masses greater than 20 GeV, and increases up to 25% for smaller dimuon masses.

In order to extract the signal from data, a simultaneous binned maximum likelihood fit is performed to the dimuon mass distributions in the two event categories. A parametric function is used to model the shape of the background. The parameters of this function and the background yield are allowed to float freely in the fit, and are uncorrelated between the two event categories. In the search using the standard triggers, the fit is performed in a dimuon mass range of $\pm 7\sigma$ around the probed resonance mass, where σ is the mass resolution parameter of the dCB function used to model the signal. The background, which is dominated by Drell-Yan events, is modeled in both event categories using the product of a modified form of the Breit-Wigner function [32] and a second order Bernstein polynomial. In the search using the scouting triggers, the fit is performed in a $\pm 5\sigma$ dimuon mass window around the probed res-

onance mass. The background mass distribution is modeled using a fourth order Bernstein polynomial. Figure 1 (inset) shows, as an example, the dimuon mass distribution of events in the barrel category in the $23.9 - 26.1$ GeV window that is used to search for a 25 GeV resonance. A fit performed to this data assuming no signal is also shown along with the expected signal due to a 25 GeV dark photon with $\epsilon^2 = 4 \times 10^{-5}$.

In order to assess the possible bias in the measurement of a signal due to the choice of the function used to model the background distribution, we consider several alternate functions that fit the data well. A test function is fit to the data in each event category, and is then used to generate 2000 sets of pseudo-data. A certain amount of signal is injected in each of the pseudo-data sets. A signal-plus-background fit is performed to each of the pseudo-data sets with the signal yield allowed to float freely. The bias is quantified as the ratio of the difference between the measured and injected signals, and the statistical uncertainty in the measured signal yield. The bias is found to be less than 10% of the statistical uncertainty in the measured signal yield for resonance masses greater than 20 GeV, in both event categories. For masses less than 20 GeV, the bias is estimated to be less than 20 (30)% for the barrel (forward) categories. In order to account for this uncertainty, we introduce an additional background in the fit. The shape of the background is taken to be the same as that of the signal, and its normalization is treated as a nuisance parameter with mean value zero, whose variations are constrained by a Gaussian distribution with standard deviation equal to the bias found in the tests.

The statistical analysis is performed using a profile likelihood test statistic in which systematic uncertainties are modeled as constrained nuisance parameters. The nuisance parameters for the dimuon mass scale and resolution uncertainties, and the bias due to the choice of the background fit function are modeled using the Gaussian probability density function. All other sources of systematic uncertainty affect the signal yield, and are modeled with nuisance parameters that are constrained using the log-normal probability density function.

The data are found to be consistent with the background expectation. Figure 2 shows the 95% confidence level (CL) upper limits on the product of the signal cross section, branching fraction to a pair of muons, and acceptance for a narrow resonance using an asymptotic approximation [33] of the CL_s method [34]. In the analysis performed with data from standard triggers, a signal event is considered to be within acceptance if each muon has $p_T > 10\,\text{GeV}$ and $|\eta| < 1.9$, and the highest-p_T muon has $p_T > 20\,\text{GeV}$. In the analysis performed with scouting data, a signal event is considered to be within acceptance if each muon has $p_T > 4\,\text{GeV}$ and $|\eta| < 1.9$. Furthermore, the (second) highest-p_T muon is required to have $p_T >$ (dimuon mass)/3(4).

The results of this search are interpreted in the context of the dark photon model. The dark photon signal process is kinematically similar to the SM Drell-Yan process. Therefore, an NLO k-factor has been computed for the signal by comparing the NLO and LO Drell-Yan cross sections, and has been found to be 1.09 over the entire mass range under consideration. A 10% uncertainty has been conservatively ascribed to the missing higher order corrections to the signal cross section. The uncertainty in the modeling of the parton distribution functions is estimated to be 2%. We set 90% CL upper limits on ϵ^2 as a function of the Z_D mass, as shown in Figure 3. These limits are compared with recent results from the LHCb Collaboration [9] and with constraints from the measurements of the electroweak observables [4].

We have presented a search for a narrow resonance decaying to a pair of muons using proton-proton collision data recorded by the CMS experiment at $\sqrt{s} = 13\,\text{TeV}$. The search in the 45–75 and 110–200 GeV resonance mass ranges uses fully reconstructed data, containing a pair of muons with transverse momenta greater than 20 and 10 GeV, and corresponding to an integrated luminosity of 137 fb^{-1}. The search in the resonance mass range of 11.5–45.0 GeV is

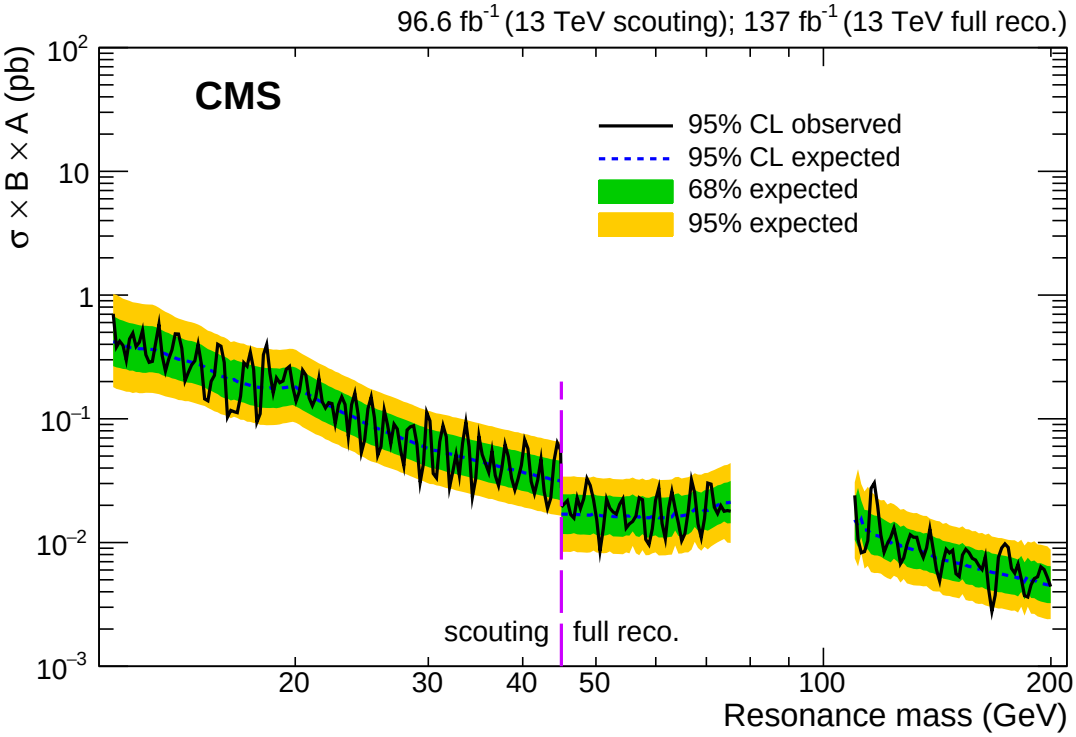

Figure 2: Expected and observed 95% CL upper limits on the product of the signal cross section (σ), branching fraction to a pair of muons (B), and acceptance (A) as a function of the mass of a narrow resonance. Results obtained using scouting data are to the left of the vertical dashed purple line, whereas results obtained using data from the standard triggers are to the right.

performed using data collected with a set of high rate dimuon triggers, corresponding to an integrated luminosity of 96.6 fb^{-1}. This is the first search that uses data with reduced trigger level muon information, collected with dimuon scouting triggers that have significantly lower transverse momentum thresholds compared to the ones used to collect data for complete reconstruction. The data are found to be consistent with the background prediction. The search sets the strongest constraints to date on the kinetic mixing coefficient of a dark photon with mass greater than 11.5 GeV.

Acknowledgments

We congratulate our colleagues in the CERN accelerator departments for the excellent performance of the LHC and thank the technical and administrative staffs at CERN and at other CMS institutes for their contributions to the success of the CMS effort. In addition, we gratefully acknowledge the computing centres and personnel of the Worldwide LHC Computing Grid for delivering so effectively the computing infrastructure essential to our analyses. Finally, we acknowledge the enduring support for the construction and operation of the LHC and the CMS detector provided by the following funding agencies: BMBWF and FWF (Austria); FNRS and FWO (Belgium); CNPq, CAPES, FAPERJ, FAPERGS, and FAPESP (Brazil); MES (Bulgaria); CERN; CAS, MoST, and NSFC (China); COLCIENCIAS (Colombia); MSES and CSF (Croatia); RPF (Cyprus); SENESCYT (Ecuador); MoER, ERC IUT, PUT and ERDF (Estonia); Academy of Finland, MEC, and HIP (Finland); CEA and CNRS/IN2P3 (France); BMBF, DFG, and HGF

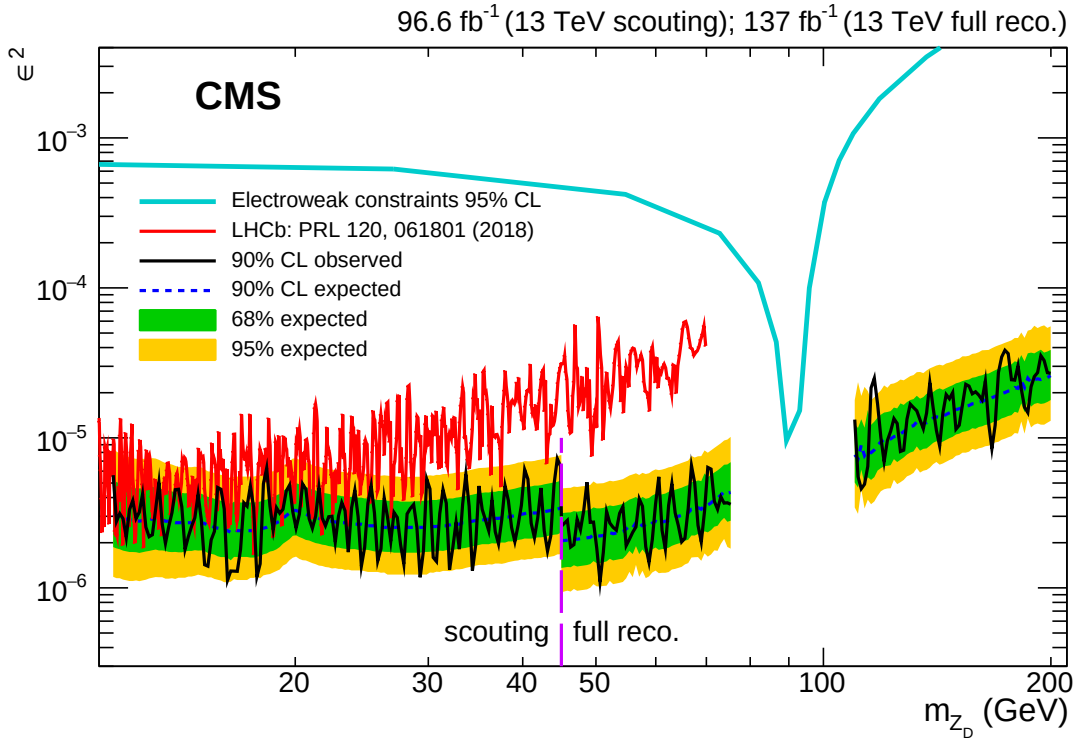

Figure 3: Expected and observed 90% CL upper limits on ϵ^2 as a function of the Z_D mass. Results obtained using scouting data are to the left of the vertical dashed purple line, whereas results obtained using data from the standard triggers are to the right. Limits from the dark photon search performed by the LHCb Collaboration [9] are shown in red, and 95% CL constraints from the measurements of the electroweak observables, are shown in light blue [4].

(Germany); GSRT (Greece); NKFIA (Hungary); DAE and DST (India); IPM (Iran); SFI (Ireland); INFN (Italy); MSIP and NRF (Republic of Korea); MES (Latvia); LAS (Lithuania); MOE and UM (Malaysia); BUAP, CINVESTAV, CONACYT, LNS, SEP, and UASLP-FAI (Mexico); MOS (Montenegro); MBIE (New Zealand); PAEC (Pakistan); MSHE and NSC (Poland); FCT (Portugal); JINR (Dubna); MON, RosAtom, RAS, RFBR, and NRC KI (Russia); MESTD (Serbia); SEIDI, CPAN, PCTI, and FEDER (Spain); MOSTR (Sri Lanka); Swiss Funding Agencies (Switzerland); MST (Taipei); ThEPCenter, IPST, STAR, and NSTDA (Thailand); TUBITAK and TAEK (Turkey); NASU and SFFR (Ukraine); STFC (United Kingdom); DOE and NSF (USA).

References

[1] P. Galison and A. Manohar, "Two Z's or not two Z's?", *Phys. Lett. B* **136** (1984) 279, doi:10.1016/0370-2693(84)91161-4.

[2] B. Holdom, "Two U(1)'s and ϵ charge shifts", *Phys. Lett. B* **166** (1986) 196, doi:10.1016/0370-2693(86)91377-8.

[3] K. R. Dienes, C. F. Kolda, and J. March-Russell, "Kinetic mixing and the supersymmetric gauge hierarchy", *Nucl. Phys. B* **492** (1997) 104, doi:10.1016/S0550-3213(97)80028-4,10.1016/S0550-3213(97)00173-9, arXiv:hep-ph/9610479.

[4] D. Curtin, R. Essig, S. Gori, and J. Shelton, "Illuminating dark photons with high-energy colliders", *JHEP* **02** (2015) 157, doi:10.1007/JHEP02(2015)157, arXiv:1412.0018.

[5] A. Konaka et al., "Search for neutral particles in electron-beam-dump experiment", *Phys. Rev. Lett.* **57** (1986) 659, doi:10.1103/PhysRevLett.57.659.

[6] APEX Collaboration, "Search for a new gauge boson in electron-nucleus fixed-target scattering by the APEX Experiment", *Phys. Rev. Lett.* **107** (2011) 191804, doi:10.1103/PhysRevLett.107.191804, arXiv:1108.2750.

[7] SINDRUM I Collaboration, "Search for weakly interacting neutral bosons produced in π^- p interactions at rest and decaying into e^+ e^- pairs", *Phys. Rev. Lett.* **68** (1992) 3845, doi:10.1103/PhysRevLett.68.3845.

[8] BaBar Collaboration, "Search for dimuon decays of a light scalar boson in radiative transitions Upsilon $\rightarrow$ gamma A0", *Phys. Rev. Lett.* **103** (2009) 081803, doi:10.1103/PhysRevLett.103.081803, arXiv:0905.4539.

[9] LHCb Collaboration, "Search for dark photons produced in 13 TeV pp collisions", *Phys. Rev. Lett.* **120** (2018) 061801, doi:10.1103/PhysRevLett.120.061801, arXiv:1710.02867.

[10] CMS Collaboration, "The CMS experiment at the CERN LHC", *JINST* **3** (2008) S08004, doi:10.1088/1748-0221/3/08/S08004.

[11] CMS Collaboration, "The CMS trigger system", *JINST* **12** (2017) P01020, doi:10.1088/1748-0221/12/01/P01020, arXiv:1609.02366.

[12] S. Mukherjee, "Data Scouting : A New Trigger Paradigm. Data Scouting : A New Trigger Paradigm", *5th Large Hadron Collider Physics Conference (LHCP 2017) Shanghai, China* (Aug, 2017).

[13] S. Gopalakrishna, S. Jung, and J. D. Wells, "Higgs boson decays to four fermions through an abelian hidden sector", *Phys. Rev. D* **78** (2008) 055002, doi:10.1103/PhysRevD.78.055002, arXiv:0801.3456.

[14] J. Alwall et al., "The automated computation of tree-level and next-to-leading order differential cross sections, and their matching to parton shower simulations", *JHEP* **07** (2014) 079, doi:10.1007/JHEP07(2014)079, arXiv:1405.0301.

[15] T. Sjöstrand et al., "An Introduction to PYTHIA 8.2", *Comput. Phys. Commun.* **191** (2015) 159, doi:10.1016/j.cpc.2015.01.024, arXiv:1410.3012.

[16] CMS Collaboration, "Event generator tunes obtained from underlying event and multiparton scattering measurements", *Eur. Phys. J. C* **76** (2016) 155, doi:10.1140/epjc/s10052-016-3988-x, arXiv:1512.00815.

[17] CMS Collaboration, "Extraction and validation of a new set of CMS PYTHIA8 tunes from underlying-event measurements", (2019). arXiv:1903.12179. Submitted to Eur. Phys. J. C.

[18] M. L. Mangano, M. Moretti, F. Piccinini, and M. Treccani, "Matching matrix elements and shower evolution for top-quark production in hadronic collisions", *JHEP* **01** (2007) 013, doi:10.1088/1126-6708/2007/01/013, arXiv:hep-ph/0611129.

[19] R. Frederix and S. Frixione, "Merging meets matching in MC@NLO", *JHEP* **12** (2012) 061, doi:10.1007/JHEP12(2012)061, arXiv:1209.6215.

[20] NNPDF Collaboration, "Parton distributions for the LHC Run II", *JHEP* **04** (2015) 040, doi:10.1007/JHEP04(2015)040, arXiv:1410.8849.

[21] NNPDF Collaboration, "Parton distributions from high-precision collider data", *Eur. Phys. J. C* **77** (2017) 663, doi:10.1140/epjc/s10052-017-5199-5, arXiv:1706.00428.

[22] S. Agostinelli et al., "Geant4 : a simulation toolkit", *Nucl. Instrum. Meth. A* **506** (2003) 250, doi:https://doi.org/10.1016/S0168-9002(03)01368-8.

[23] CMS Collaboration, "Particle-flow reconstruction and global event description with the CMS detector", *JINST* **12** (2017) P10003, doi:10.1088/1748-0221/12/10/P10003, arXiv:1706.04965.

[24] M. Cacciari, G. P. Salam, and G. Soyez, "The anti-k_t jet clustering algorithm", *JHEP* **04** (2008) 063, doi:10.1088/1126-6708/2008/04/063, arXiv:0802.1189.

[25] M. Cacciari, G. P. Salam, and G. Soyez, "FastJet user manual", *Eur. Phys. J. C* **72** (2012) 1896, doi:10.1140/epjc/s10052-012-1896-2, arXiv:1111.6097.

[26] CMS Collaboration, "Identification of heavy-flavour jets with the CMS detector in pp collisions at 13 TeV", *JINST* **13** (2018) P05011, doi:10.1088/1748-0221/13/05/P05011, arXiv:1712.07158.

[27] CMS Collaboration, "Performance of the CMS muon detector and muon reconstruction with proton-proton collisions at $\sqrt{s} = 13$ TeV", *JINST* **13** (2018) P06015, doi:10.1088/1748-0221/13/06/P06015, arXiv:1804.04528.

[28] M. J. Oreglia, "A study of the reactions $\psi' \to \gamma\gamma\psi$", (1984). Ph.D. thesis, Stanford University. SLAC Report SLAC-R-236.

[29] CMS Collaboration, "CMS Luminosity Measurements for the 2016 Data Taking Period", Technical Report CMS-PAS-LUM-17-001, CERN, Geneva, 2017.

[30] CMS Collaboration, "CMS luminosity measurement for the 2017 data-taking period at $\sqrt{s} = 13$ TeV", Technical Report CMS-PAS-LUM-17-004, CERN, Geneva, 2018.

[31] CMS Collaboration, "CMS luminosity measurement for the 2018 data-taking period at $\sqrt{s} = 13$ TeV", Technical Report CMS-PAS-LUM-18-002, CERN, Geneva, 2019.

[32] CMS Collaboration, "Search for the Higgs boson decaying to two muons in proton-proton collisions at $\sqrt{s} = 13$ TeV", *Phys. Rev. Lett.* **122** (2019), no. 2, 021801, doi:10.1103/PhysRevLett.122.021801, arXiv:1807.06325.

[33] G. Cowan, K. Cranmer, E. Gross, and O. Vitells, "Asymptotic formulae for likelihood-based tests of new physics", *Eur. Phys. J. C* **71** (2011) 1554, doi:10.1140/epjc/s10052-011-1554-0, 10.1140/epjc/s10052-013-2501-z, arXiv:1007.1727. [Erratum: Eur. Phys. J.C73,2501(2013)].

[34] A. L. Read, "Presentation of search results: the CL_s technique", *J. Phys. G* **28** (2002) 2693, doi:10.1088/0954-3899/28/10/313.